

Article

Synthesis, Characterization and Antibacterial Efficacy of *Catharanthus roseus* and *Ocimum tenuiflorum*-Mediated Silver Nanoparticles: Phytonanotechnology in Disease Management

Acharya Balkrishna ¹, Naveen Thakur ^{2,*}, Bhavana Patial ², Saurabh Sharma ³, Ashwani Kumar ^{1,*} , Vedpriya Arya ^{1,4} and Ryszard Amarowicz ⁵ 

¹ Patanjali Herbal Research Department, Patanjali Research Institute, Haridwar 249405, India

² Department of Physics, Career Point University, Hamirpur 176041, India

³ Department of Chemistry, Career Point University, Hamirpur 176041, India

⁴ Centre of Excellence, Patanjali Ayurved Hospital, Haridwar 249405, India

⁵ Institute of Animal Reproduction and Food Research, Polish Academy of Sciences, 10-748 Olsztyn, Poland; r.amarowicz@pan.olsztyn.pl

* Correspondence: naveen.phy@cpuh.in (N.T.); dr.ashwanikumar@patanjali.res.in (A.K.)

Abstract: Nanotechnology is an emerging multidisciplinary field that has the potential to offer solutions to pharmaceutical challenges starting from drug delivery to therapeutic applications. The plant-mediated method is eco-friendly and the most inexpensive of the various techniques used to synthesize nanoparticles (NPs). In this study, silver (Ag) NPs have been successfully synthesized using leaf extract of *Catharanthus roseus* and *Ocimum tenuiflorum*. X-ray diffraction revealed an average crystalline size of 19.96 and 21.42 nm for *C. roseus* and *O. tenuiflorum*-mediated Ag NPs, respectively. Further, shape, size, and elemental composition were analyzed using a scanning electron microscope, transmission electron microscope (TEM), and energy-dispersive X-ray spectral technique. TEM study revealed spherical/spheroidal-shaped Ag NPs were formed between 10–48 nm with *C. roseus* and 17–55 nm with *O. tenuiflorum*. Both synthesized Ag NPs inhibited *Escherichia coli* and *Bacillus subtilis*, where the effect was more prominent against *E. coli* (MIC $3.90 \pm 0 \mu\text{g/mL}$) with *O. tenuiflorum* Ag NPs. Mechanistic insights of antibacterial activity were also highlighted, and the activity might be attributed to the diverse mode of action of surface functionalized phytoconstituents and NPs.

Keywords: green synthesis; silver nanoparticles; *Catharanthus roseus*; *Ocimum tenuiflorum*; Antibacterial mechanism



Citation: Balkrishna, A.; Thakur, N.; Patial, B.; Sharma, S.; Kumar, A.; Arya, V.; Amarowicz, R. Synthesis, Characterization and Antibacterial Efficacy of *Catharanthus roseus* and *Ocimum tenuiflorum*-Mediated Silver Nanoparticles: Phytonanotechnology in Disease Management. *Processes* **2023**, *11*, 1479. <https://doi.org/10.3390/pr11051479>

Academic Editors: Douglas J. H. Shyu, Yih-Yuan Chen, Sechul Chun

Received: 1 March 2023

Revised: 5 May 2023

Accepted: 10 May 2023

Published: 12 May 2023



Copyright: © 2023 by the authors. Licensee MDPI, Basel, Switzerland. This article is an open access article distributed under the terms and conditions of the Creative Commons Attribution (CC BY) license (<https://creativecommons.org/licenses/by/4.0/>).

1. Introduction

Nanotechnology is one of modern science's most promising research areas, affecting all spheres of human life [1]. It entails the usage of 1–100 nm size range particles known as nanoparticles (NPs). Numerous approaches can be used to synthesize NPs, such as chemical, physical, biological, and hybrid methods [2]. Chemical processes are widely explored and utilized in various NPs formations with toxic chemicals, whereas physical methods require high energy and sophisticated instruments. Hence, there is a growing need to develop an eco-friendly or alternative method for synthesizing NPs. In this context, biological, or green processes are preferred as they are eco-friendly and cost-effective [3–6]. Using biological organisms, green nanotechnology allows us to break all barriers of high energy consumption, low yield, imperfect surface structure, etc. Green synthesis is economical, biocompatible, and safe as it mediates through plants, fungi, algae, bacteria, actinomycetes, and other organisms [7,8]. In comparison to conventional methods, bacteria, fungi, and natural products contain abundant hydrogen (H⁺) atoms that play a significant role in the synthesis of NPs [9,10]. For example, the green synthesized Fe₃O₄ NPs possessed a size range of 2–80 nm, which is quite smaller than the chemically

synthesized NPs with a size range of 87–400 nm [11]. In addition, this method does not require toxic solvents, the addition of reducing agents, or a high temperature [12]. The biological precursors of metallic NPs can act as a reducing agent that undergoes nucleation of atomized metal ions and forms metallic NPs in aqueous solutions [13]. Certain metal-resisting bacterial species possess the potential to reduce metal ions and form desired inorganic metallic NPs through their active functional groups [14,15]. These microorganisms secrete some significant reductase enzymes such as nitrate reductase and α -NADPH-dependent reductases, and act as reducing agents for synthesizing metallic NPs [16]. For instance, the supernatant of *Pseudomonas aeruginosa* ATCC 90271 bacterial strain was used to synthesize gold (Au) NPs of with a size range between 15–40 nm [17]. Similarly, the yeast and non-phototrophic fungi that secrete some functional proteins could fabricate metal NPs from aqueous M^+ ions [18,19]. For example, Au and silver (Ag) NPs have been synthesized using the yeast *Candida guilliermondii* and tested for antimicrobial activity against pathogenic bacterial strains [20]. Compared to a microbial technique that requires time-consuming and expensive downstream processing, phyto-mediated synthesis is advantageous [21–23].

Subsequently, very few reports supported the use of algal extract as a reductant source because of the absence of a well-developed cellular structure and the maintenance of cellular media. Therefore, to overcome this limitation, higher plants with medicinal value are widely explored as compared with algae or lower plants and break this barrier in the field of nanoscience [24,25]. When compared with microorganisms, plants are easily accessible biological resources that produce a higher amount of reducing agents in their different parts such as root, leaves, stem, and flowers [26]. The presence of secondary metabolites such as polyphenols, alkaloids, terpenoids, glycosides, alcohols, carbohydrates, ascorbic acid, flavonoids, and phenolic acids helps the reduction of metal ions into metallic NPs form. For example, an extract of *Pogestemon benghalensis* was used to synthesize gold nanoparticles, which are triangular or spherical and show a size range of 10–50 nm [27]. Further, under stress conditions plants produce a variety of secondary metabolites such as polyphenols and terpenes that can convert metal ions into NPs [28]. Plants also generate phytochelatin, metallothioneins, and peptides as chelating agents to create less toxic or stable complexes with carbonyl or hydroxyl groups for detoxification in metal-stressed circumstances [29].

NPs such as copper, titanium, gold, zinc, silver, cadmium, iron, etc. have been explored in the literature with different approaches [30–33]. Among all these, Ag NPs are the most significant because of their unique properties and applications, such as antimicrobial, chemical stability, conductivity, etc. [6,34]. Further, it has been reported that Ag NPs are most efficient against bacteria, viruses, and other microorganisms even at low concentrations [35,36]. The attachment of plant bioactive molecules on the surface of NPs has been associated with increased biological potential [22]. In a standard protocol, Ag NPs are synthesized using silver nitrate (as a precursor) and plant extract under a specific temperature and pH [37,38]. The flavonoids in the extracts reduce the NPs and stabilize them. The color change confirms their synthesis [39]. Various applications for these NPs can be found in medicine, catalysis, optics, and energy. Their antibacterial properties make them an ideal ingredient in ointments for treating burns and wounds and coatings for surgical masks and implantable devices [40].

Ag NPs have been synthesized using a variety of plants with variable sizes and shapes, and their biological activity varies significantly, which might be due to plant selection. The selection of plants with bioactive molecules is crucial for synthesis and biomedical applications. Additionally, the phytoconstituents of plants vary with altitude, which will also affect size, shape, and biological activity. Himalayan region plants are rich in bioactive composition, so the present study is designed to synthesize Ag NPs using leaf extracts of *Catharanthus roseus* (L.) G. Don and *Ocimum tenuiflorum* L. *C. roseus*, commonly known as Madagascar periwinkle, is a member of the family *Apocynaceae*. It is native to Madagascar [41]. *C. roseus* has several applications in traditional medicine, especially for

diabetes and cancer [42]. Its bioactive composition includes phenols, flavonoids, tannins, and alkaloids content. The higher phenols and flavonoid concentrations in leaf extract were 0.65 ± 0.02 and 0.62 ± 0.02 $\mu\text{g}/\text{mL}$, respectively [43]. *O. tenuiflorum*, belonging to the family *Lamiaceae*, is widely distributed from tropical and subtropical Asia to the Western Pacific region [41]. In Ayurveda, it has been used for treating several ailments and is reported to be a stimulant and antipyretic herb. Phenolic compounds, flavonoids, phenylpropanoids, coumarins, tannins, and terpenoids are the bioactive molecules of *O. tenuiflorum* [44]. The total polyphenolic and flavonoid contents of *O. tenuiflorum* leaves were 212.26 ± 6.3 mg GAE/g extract and 54.51 ± 3.5 mg QE/g extract, respectively [45]. Drug resistance and emerging pathogens have made the search for novel antibacterials inevitable. NPs have been reported to be strong antimicrobials, so we are also endeavoring to evaluate the antibacterial potential of synthesized Ag NPs.

2. Materials and Methods

2.1. Materials

Silver nitrate (Merck) was procured and used without any purification. Leaves of *O. tenuiflorum* and *C. roseus* were collected from Career Point University, Hamirpur (1189 m), Himachal Pradesh, India. The plants were authenticated by the scientists of the Herbal Research Division, Patanjali Research Institute, Haridwar, India. No specific authorization was required for collecting plant parts because they are not protected by national or international laws. *Escherichia coli* and *Bacillus subtilis* were procured from Microbial Type Culture Collection and Gene Bank, IMTECH, Chandigarh, India.

2.2. Preparation of Plant Extracts

Fresh leaves (20 g) of *C. roseus* and *O. tenuiflorum* were washed well with distilled water to remove impurities/dust. Leaves were finely cut and ground in mortar and pestle, followed by 10 min of boiling in 100 mL of double distilled water. After cooling, the resultant mixture was filtered to eliminate particulates and used to synthesize Ag NPs.

2.3. Synthesis of Silver NPs

Ag NPs were synthesized as per the methodology described earlier by Kuppurangan et al. [46] with modifications. The aqueous solution of silver nitrate (10 mM) was prepared, and 10 mL of plant extract was added dropwise to it under constant stirring with a magnetic stirrer. The solution was kept under a stirrer until the color of the solution changes to dark brown, indicating the formation of Ag NPs. Further, the solution was undisturbed for 2 days so that the NPs settle down at the bottom (Figure 1). The obtained NPs were dried at 60°C after successive washing with double distilled water and lastly with ethanol. A yield of ≈ 45 mg was recovered from the reaction of 100 mL.

2.4. Characterization of the NPs

NPs were characterized as per the methodology described earlier by various researchers [31,33,47]. The synthesized NPs were characterized by X-ray diffraction (XRD) method for the crystallinity and phase study of the prepared samples using SmartLab 9 kW rotating anode X-ray diffractometer (Rigaku Corporation) in the diffraction angles (2θ) from 20° to 80° (scanning range) at $20^\circ/\text{min}$ scanning rate. FEI Quanta FEG-450 (FEI, USA) scanning electron microscope (SEM) and energy dispersive X-ray spectroscopy (EDS or EDX) were used to study the external morphology and elemental analysis of Ag NPs. The shape and size were examined by FP 5022/22-Tecnai G2 20 S-TWIN (FEI, USA) transmission electron microscope (TEM). Lastly, the FTIR spectroscopy of NPs was performed from 4000 to 400 cm^{-1} spectrum range using Cary, 630 FTIR (Agilent Technologies, India).



Figure 1. Experimental design for synthesis of Ag NPs using *O. tenuiflorum* and *C. roseus*.

2.5. Nanoparticles Preparation for Antibacterial Study

A stock solution of NPs with a final concentration of 1000 $\mu\text{g}/\text{mL}$ was prepared in methanol and kept at 4 $^{\circ}\text{C}$ for later use. The stock solution was sonicated for 15 min at 25 $^{\circ}\text{C}$ before experimental usage.

2.6. Antibacterial Activity

2.6.1. Well Diffusion Assay

The preliminary antibacterial efficacy of Ag NPs was evaluated using a modified well diffusion assay [48]. Mueller Hinton agar (MHA) were prepared and used for well diffusion assay. Each inoculum (*Escherichia coli* and *Bacillus subtilis*) was applied with a sterile cotton swab, on the whole surface of the corresponding MHA plates. Wells were then made into plates using a cork borer. Ag NPs (250, 500 and 1000 $\mu\text{g}/\text{mL}$ *w/v*) were loaded into the wells. Tetracycline (25 $\mu\text{g}/\text{mL}$ *w/v*) served as the positive control, and methanol was used as the negative control. The zone of inhibition was measured using the Hi antibiotic zone scale following incubation for 24 h at 37 $^{\circ}\text{C}$.

2.6.2. Minimum Inhibitory Concentration and Minimum Bactericidal Concentration of Ag NPs

The minimum inhibitory concentration (MIC) of Ag NPs was performed using the broth microdilution method [49]. Firstly, the inoculums were prepared and standardized with 0.5 McFarland standard ($1\text{--}2 \times 10^8$ CFU/mL). Secondly, wells were made in the Mueller Hinton agar (MHA) plates containing bacterial inoculums and different conc. (250, 500, and 1000 $\mu\text{g}/\text{mL}$ *w/v*) of Ag NPs were filled in wells followed by 24 h incubation at 37 $^{\circ}\text{C}$. Tetracycline (25 $\mu\text{g}/\text{mL}$ *w/v*) and methanol were used as the positive and negative control, respectively. Thirdly, in MIC determination, 96 wells of microtiter plate were aliquoted with Muller Hinton Broth (MHB, 100 μL of 2X conc.). Briefly, Ag NPs (100 μL of 2X conc.) were added in the first well, and successive dilutions (250–0.97 $\mu\text{g}/\text{mL}$) were prepared up to the ninth well. After that, each well was filled with 10 μL inoculum. The 10th and 11th wells were used as negative (inoculum, MHB, and methanol) and positive control (Tetracycline, MHB, and inoculum), respectively. The 12th well with MHB and inoculum was used as a growth control well. The MIC was the lowest concentration at which growth inhibition was initiated. In addition, after transferring 10 μL of suspension from microtiter plate on the agar plates, minimum bactericidal concentration (MBC) was considered with no colonies.

2.7. Statistical Analysis

The experiments were conducted in triplicates for antibacterial activity, and average and standard deviation were determined using GraphPad Prism.

3. Results and Discussion

3.1. XRD Analysis

XRD analysis was conducted to determine the crystal structure of Ag NPs. Figure 2 a gives the XRD diffraction patterns of *C. roseus*-mediated Ag NPs. The values of 2θ were taken between 20 to 80 degrees. Four different diffraction peaks at 38.18, 44.28, 64.55, and 77.46° are indexed corresponding to the planes (111), (200), (220), and (311), respectively [50]. These planes confirmed that the crystal structures of synthesized Ag NPs are face-centered cubic in nature. The lattice constant 'a' values corresponding to these angles are 4.085, 4.086, 4.075, and 4.079, respectively. Similar diffraction peaks (Figure 2b) also govern the formation of (111), (200), (220), and (311) planes for *O. tenuiflorum* Ag NPs. The lattice constant 'a' values corresponding to these angles/planes are 4.077, 4.067, 4.073, and 4.079, respectively. In Figure 2b, the XRD patterns recorded at 27.92, 32.31, 46.27, 54.92, and 57.3° correspond to the occurrences of the Ag₂O₃ crystalline structure. Janardhanan et al. [51] reported similar observations with Ag NPs and silver oxide (Ag₂O) particles. These peaks were well matched with the JCPDS File No. 771829. These patterns in the spectra confirmed the plant selective synthesis and formation of Ag and Ag₂O₃ using *O. tenuiflorum*, whereas using the *C. roseus*, the formation of pure Ag crystalline NPs was observed. The average crystalline size using Scherrer's equation was found to be 19.96 and 21.42 nm for Ag NPs prepared using *C. roseus* and *O. tenuiflorum*, respectively. Scherrer's equation:

$$D = \frac{0.94\lambda}{\beta \cos \theta}$$

where

D = Average crystalline size.

β = Line broadening in radians.

θ = Bragg's angle.

λ = X-ray wavelength ($\lambda = 1.5418 \text{ \AA}$).

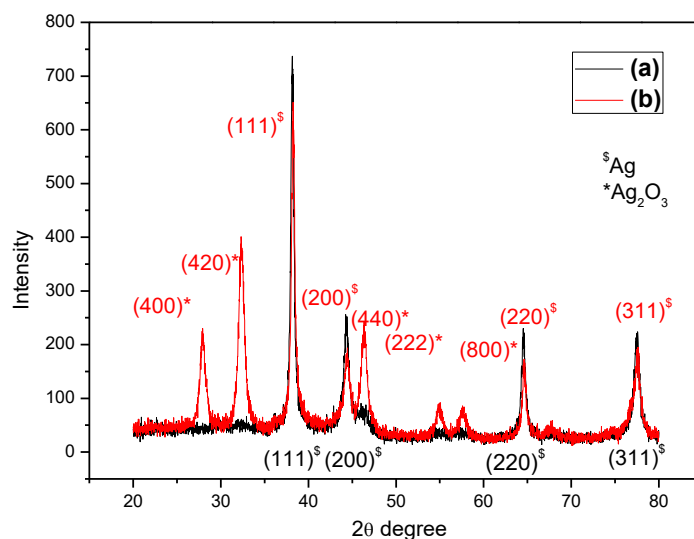


Figure 2. XRD patterns of Ag NPs synthesized using *C. roseus* (a) and *O. tenuiflorum* (b).

3.2. EDX Analysis

EDX images of synthesized Ag NPs (Figure 3) revealed that NPs are composed of silver metal only, as EDX spectra have strong signals for silver metal at 3 keV, which is

in close agreement with optical absorption peaks reported earlier [52]. In contrast, the other unassigned low-intensity peaks may correspond to the peaks of carbon and oxygen present in the sample [53]. The carbon and oxygen are supposed to represent the plant phytochemicals or biomass that take part in the stability of the Ag NPs synthesized by using the plant extract.

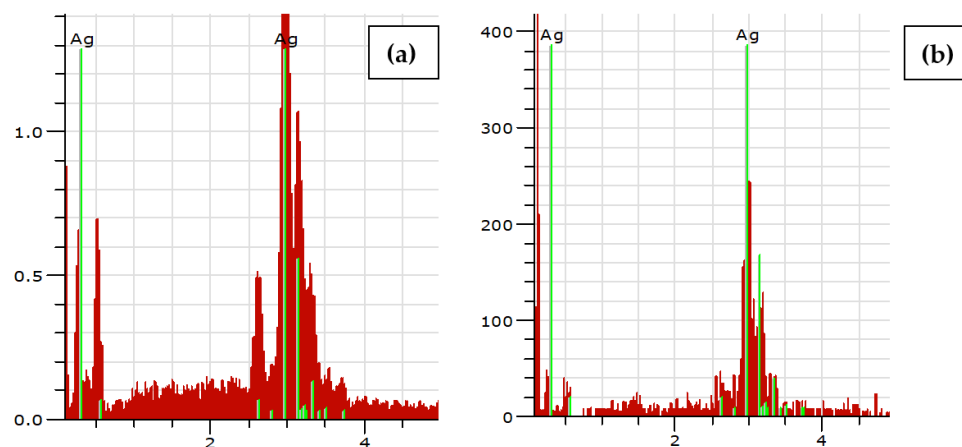


Figure 3. EDX spectra of *C. roseus* (a) and *O. tenuiflorum* (b) mediated Ag NPs.

3.3. SEM Analysis

The size, morphology, and shape of synthesized Ag NPs were analyzed by using SEM. SEM images show the formation of high-density, mostly spherical Ag NPs with sizes ranging between 30–70 nm in both cases (Figure 4). This demonstrated that the plants actively engaged in the synthesis and regulation of the formation of Ag NPs. However, the particles are found to be aggregated in both the synthesis. *Gleichenia pectinata*-mediated Ag NPs were found as aggregates of spherical shape as reported by Femi-Adepoju et al. [52]. Further, *O. tenuiflorum*, *Musa balbisiana*, and *Azadirachta indica* extracts resulted in cuboidal, spherical, and triangular Ag NPs, respectively [54]. This might be due to the diverse bioactive composition of plant extracts.

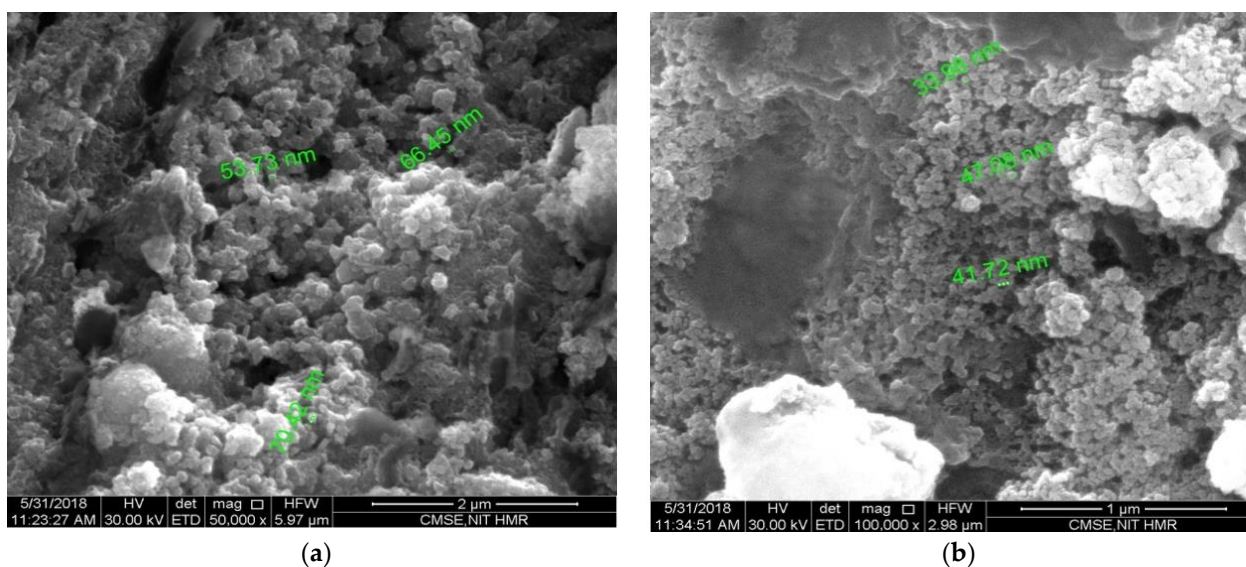


Figure 4. SEM images of Ag NPs synthesized using *C. roseus* (a) and *O. tenuiflorum* (b).

3.4. TEM Analysis

The shape and size of the Ag NPs were further examined by using TEM. The particle size of *C. roseus* mediated NPs ranged between 10–48 nm. While the size of *O. tenuiflorum*

synthesized NPs lies between 17–55 nm (Figure 5). On the contrary, the NPs synthesized using the *O. tenuiflorum* are comparatively bigger. The shape of the NPs synthesized using both plants had a similar pattern of particle formation. Most synthesized NPs were spherical/spheroidal in shape, while some were hexagonal. The same phenomenon was also seen in the crystalline size calculated by the XRD analysis. Ankamwar et al. [55] also reported the same type of morphology for Ag NPs, where the *Embllica officinalis* fruit extract was used for synthesis. In continuation, *Lippia javanica* plant extract also resulted in spheroidal-shaped Ag NPs [56]. Ahmed and Ikram [57] synthesized spherical and 8–50 nm sized Ag NPs from *Terminalia arjuna* bark. On the other hand, Kumar et al. [58] synthesized spherical shaped Ag NPs of size within 92–73 nm and 30–29 nm using seed and leaf extract and fractions of *Syzygium cumini*, respectively. Additionally, the authors observed that a decrease in polyphenols (extracts and fractions of seeds and leaves of *Syzygium cumini*) directly decreases the size of NPs. Similar to this, Saxena et al. [59] produced monodispersed, spherical-shaped Ag NPs with a size of 16.6 nm from *Ficus benghalensis* leaf extract.

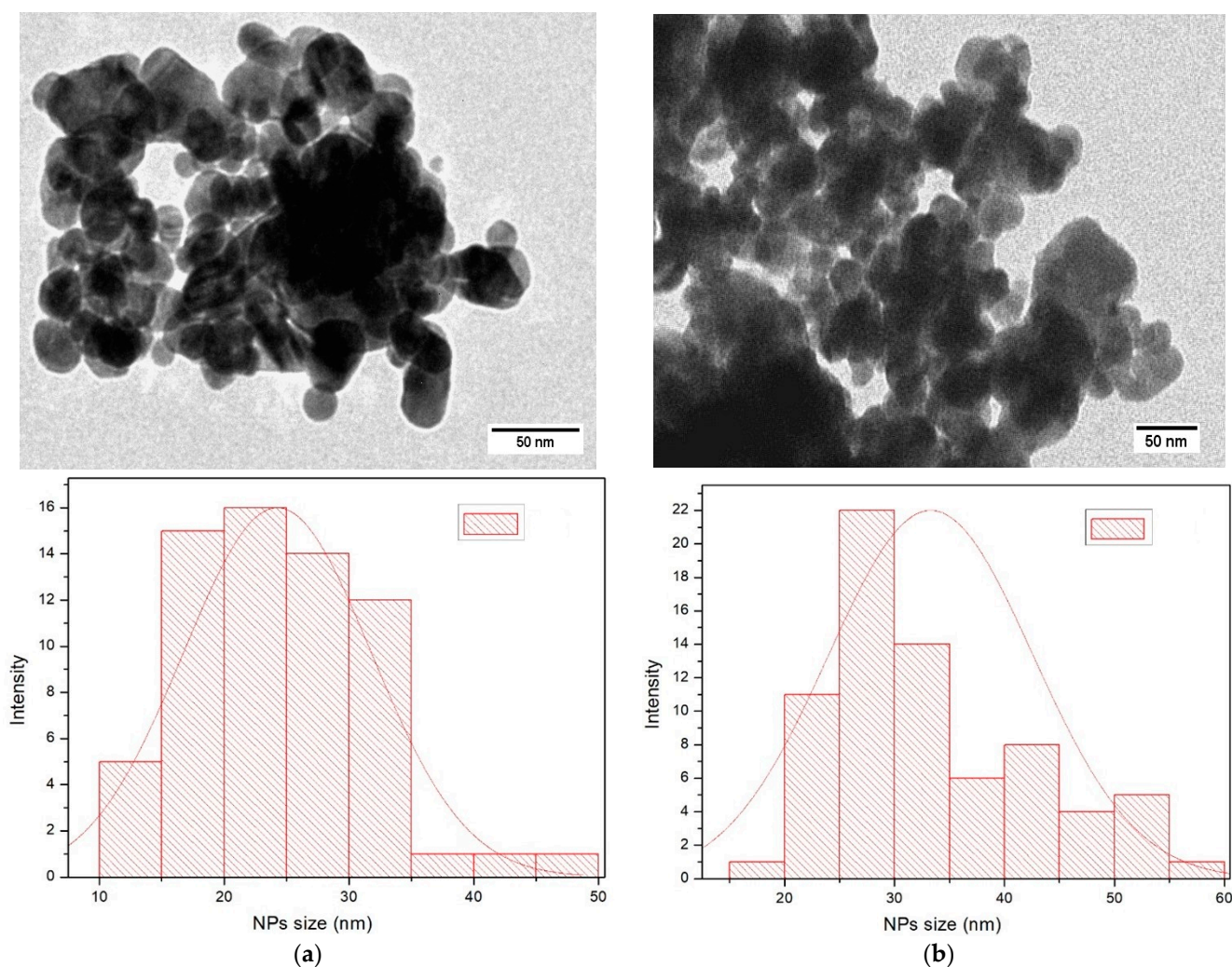


Figure 5. TEM images and particle size distribution of *C. roseus* (a) and *O. tenuiflorum* (b) mediated Ag NPs.

3.5. FTIR Analysis

The FTIR spectrum for Ag NPs is depicted in Figure 6. These spectra display numbers of absorption bands which indicate the complex nature of Ag NPs and different biomolecules of the plant extract. FTIR spectrum of *C. roseus* Ag NPs (Figure 6a) showed

the absorption bands at 2899, 2358, 1664, 1512, 1427, 1377, 1319, 1229, 1159, 1098, 1032, 899, 708, and 553 cm^{-1} which correspond to aldehydic C–H, alkene C=C, amide C=O, aromatic C=C, CH_3 , C–O–C, etc., functional groups stretching vibrations, respectively. The FTIR spectrum of *O. tenuiflorum* Ag NPs (Figure 6b) showed absorption bands at 3253, 2358, 2164, 1585, 1370, 1237, 1047, 738, 718, 644, 598, and 549 cm^{-1} which represent alcoholic OH, aldehydic C–H, C=N, amide C=O, C–O–C, etc. stretching vibrations, respectively. Ag NPs are generated by binding Ag^+ to an amide group that is present between 3300–3500 cm^{-1} (Figure 6a). The presence of an amide group, which functions as a potent reducing and capping agent, is linked to the synthesis of Ag NPs via the reduction of silver nitrate [60]. Ramteke et al. [61] reported bands of *O. sanctum*-mediated Ag NPs at 1654 and 1614 cm^{-1} which corresponds to C=C (aromatic rings) and the C–C (alkene rings), respectively, ether linkages were confirmed from bands at 1012 and 1080 cm^{-1} . Further, they revealed distinctive bands for eugenol, terpenes, and linalools of *O. sanctum* extract. Palaniappan et al. [62] reported FTIR spectra of *C. roseus*, with bands at 2927, 1680, 1460, and 980 cm^{-1} for the respective groups; however, the shifting of the band in present study governs the role surface functionalized phytochemicals that are supposed to be involved in the stabilization and capping of the Ag NPs. Similarly, the shifting in the band position for pure *O. sanctum*, reported at 2130, 1630, 1550, 1320, 1250, 1060, 1030, and 780 cm^{-1} by Mandal and Bhattacharya [63] relative to the current study also governs the same and provide the suitable evidence for the synthesis of Ag NPs by the plant extract. FTIR studies revealed that different functional groups took part in the capping and stabilization of the NPs as *C. roseus* and *O. tenuiflorum* extract have diverse phytochemicals such as alkaloids, flavonoids, phenolic compounds, and others [45,64].

3.6. Antibacterial Activity

Ag NPs synthesized using *O. tenuiflorum* and *C. roseus* inhibited *Escherichia coli* and *Bacillus subtilis*. The effect is more pronounced against *Escherichia coli* (Inhibition zone diameter 17 ± 1 and 16.6 ± 0.58 mm with *O. tenuiflorum* and *C. roseus* mediated Ag NPs) as compared to *Bacillus subtilis* in both Ag NPs types as shown in Table 1 (see Supplementary Material Figure S1 for pictorial representation).

Table 1. Antibacterial activity of *C. roseus* and *O. tenuiflorum* mediated Ag NPs.

NPs Types	Conc. ($\mu\text{g/mL}$)	Bacterial Strains					
		<i>Escherichia coli</i>			<i>Bacillus subtilis</i>		
		IZD (mm) \pm SD	MIC ($\mu\text{g/mL}$) \pm SD	MBC ($\mu\text{g/mL}$) \pm SD	IZD (mm) \pm SD	MIC ($\mu\text{g/mL}$) \pm SD	MBC ($\mu\text{g/mL}$) \pm SD
OSAg NPs	250	15.6 ± 1.15			11.3 ± 0.58		
	500	16 ± 0	3.90 ± 0	125 ± 0	12 ± 0	6.51 ± 2.26	125 ± 0
	1000	17 ± 1			13.6 ± 1.15		
CRAg NPs	250	14.3 ± 0.58			10 ± 0		
	500	14.6 ± 0.58	7.81 ± 0	250 ± 0	10.3 ± 0.58	15.6 ± 0	250 ± 0
	1000	16.6 ± 0.58			11 ± 0		

OSAg NPs: *O. tenuiflorum* mediated Ag NPs; CRAg NPs: *C. roseus* mediated Ag NPs; MIC: Minimum inhibitory concentration; IZD: Inhibition zone diameter; MBC: Minimum bactericidal concentration; SD: Standard deviation.

The well diffusion assay findings and the MIC and MBC of synthesized Ag NPs show a good correlation. The lowest MIC (3.90 ± 0 $\mu\text{g/mL}$) was observed with *O. tenuiflorum* mediated Ag NPs against *E. coli*, whereas the lowest MBC values, i.e., 125 ± 0 $\mu\text{g/mL}$, was observed against the same with both Ag NPs types. Positive control tetracycline exhibited MIC of 0.19 and 0.39 $\mu\text{g/mL}$, respectively. No activity was observed with negative control methanol. The Ag NPs synthesized from the leaves of *Anacardium occidentale* also showed potent antimicrobial activity with MIC ranges from 3.5–14.5 $\mu\text{g/mL}$ against different

microorganisms such as *E. coli* and *S. aureus* [65]. Rautela et al. [66] observed a MIC value of 2.0 µg/mL against *E. coli* with *Tectona grandis*-mediated Ag NPs. The difference in the MIC may be due to the type of bacterial strain and diversity of phytoconstituents attached to the surface of Ag NPs. Numerous studies have demonstrated that NPs were more potent antibacterials against Gram positive than Gram negative bacterial strains because the latter have a cell wall made up of LPS, lipoproteins, and phospholipids that act as a penetration barrier and only permit the entry of macromolecules [67,68].

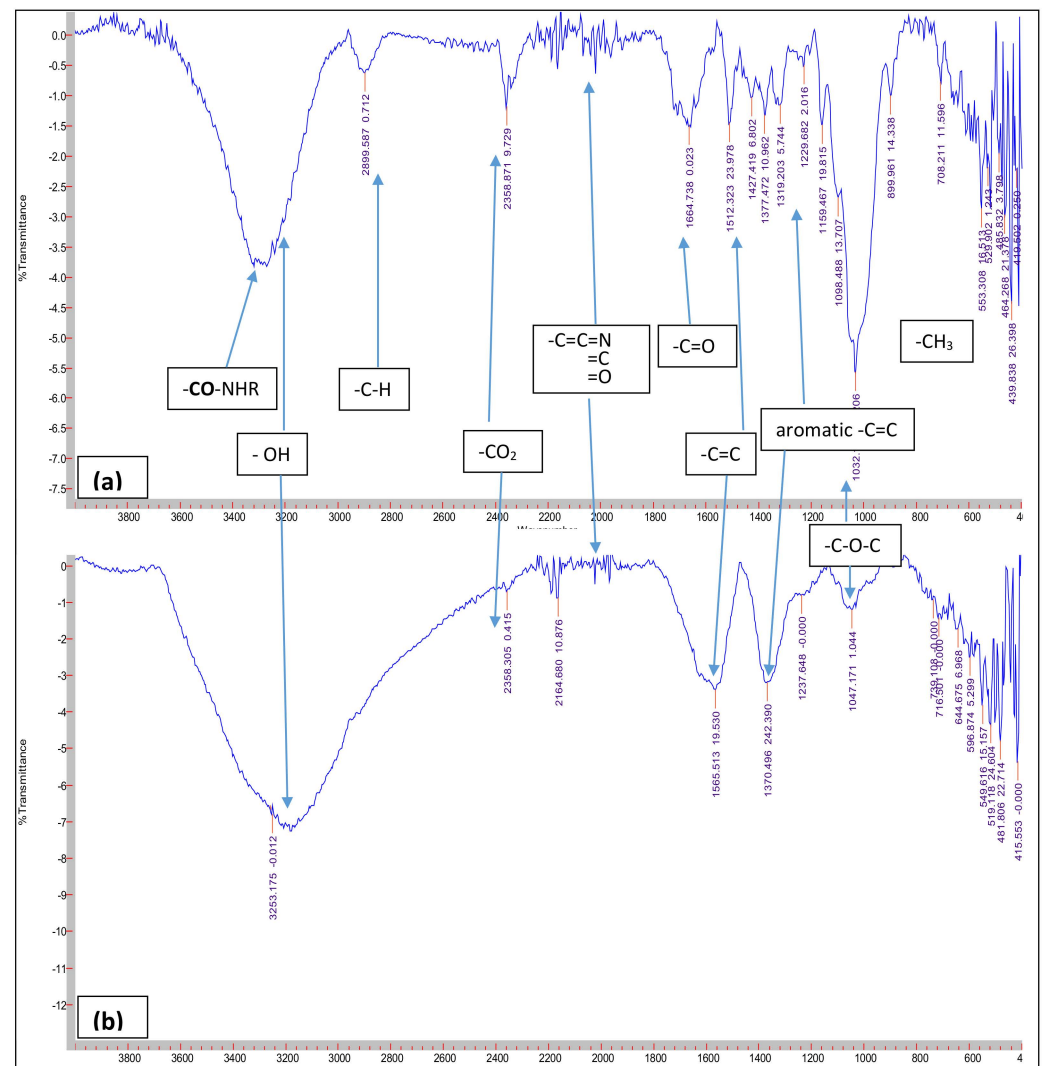


Figure 6. FTIR spectrum of Ag NPs synthesized from (a) *C. roseus* and (b) *O. tenuiflorum*.

In contrast, our study revealed that *E. coli* is more susceptible than *B. subtilis*. Additionally, Ag and Ag₂O₃ NPs were formed using *O. tenuiflorum*, Ag₂O₃ NPs can positively enhance the antibacterial potential. This fact is also supported by the existing literature where *Ficus benghalensis* prop root-mediated Ag₂O NPs showed excellent activities against the two-dental bacteria *Streptococcus mutans* and *Lactobacilli* sp. [69].

4. Mechanism of Antibacterial Activity: From Plants to NPs

In recent years, severe health issues have been caused by microorganisms' growing resistance to antibiotics. Most bacterial strains that cause infections are resistant to at least one antibiotic that is often used to treat the same. This issue inspires researchers to investigate novel compounds that can successfully inhibit microbial growth. In this context, applications of nanotechnology in microbiology and pharmaceuticals have shown

promise in combating the issue of antibiotic resistance. Different bacterial strains adopt various distinct antibiotic resistance mechanisms, such as alteration of the molecular target, overexpression of efflux pumps, biofilm formation, and enzyme-mediated modification or degradation of antibiotics, as highlighted in Figure 7 [70–73]. Plant bioactive molecules could be broad-spectrum antimicrobials owing to their diverse mode of action. They contribute significantly by acting as drug-inactivating enzyme inhibitors and preventing the efflux pump's overexpression. Moreover, they display anti-biofilm activity and inhibit protein and DNA synthesis as shown in Figure 7 [74]. Subsequently, even though several methods, inventions, and formulations have been developed over time, the specific mechanism by which NPs affect bacteria and fungi has not yet been fully established. Some reported mechanisms include direct contact and cell membrane destabilization, permeability alteration, metal ions release, reactive oxygen species generation, enzyme disruption, DNA, and protein damage [75–78].

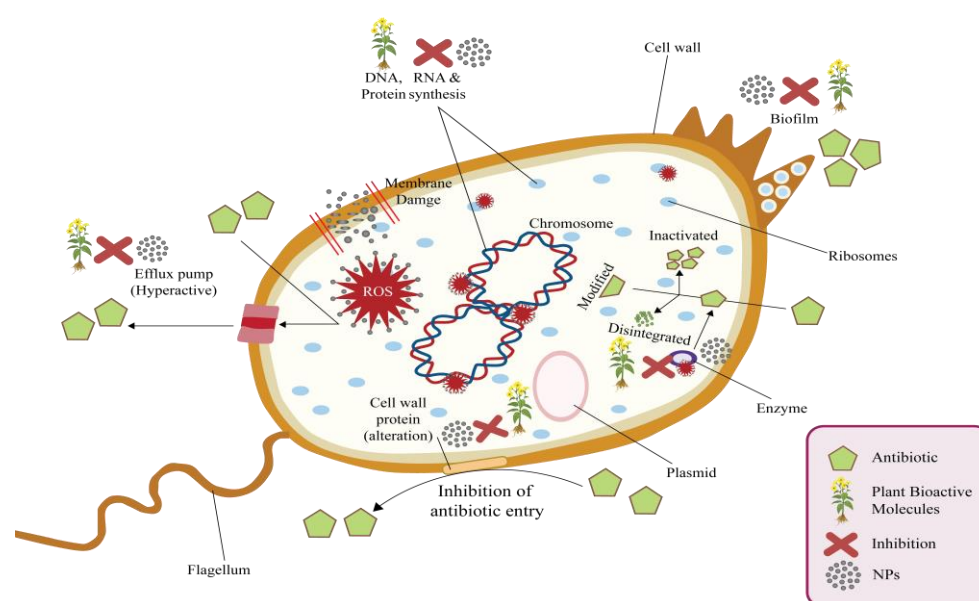


Figure 7. Insights into antibiotic resistance among bacterial strains and the impact of plant bioactive molecules and NPs against drug resistance.

The antibacterial actions of silver NPs are mediated through the release of silver ions (Ag^+) leading to disruption of the cell wall and cytoplasmic membrane, denaturing ribosomes and inhibiting protein synthesis, termination of ATP production as they deactivate respiratory enzyme on the cytoplasmic membrane. In addition, reactive oxygen species generation disrupts the membrane and binds to DNA, and inhibits replication (Figure 7). Further, Ag NPs migrate across the cytoplasmic membrane, releasing cell organelles [75,76,78–81]. Ag NPs (prepared from *Albizia lebbek* bark) can damage cell walls and membranes, resulting in several pores and leakage of cytosolic content of *Pseudomonas aeruginosa* and *Serratia marcescens* [82]. Researchers have explored several mechanisms for the mode of action of NPs including Ag NPs. Likewise, the plants and their diverse bioactive composition were found to be potent antimicrobials as various mechanisms mediate their activity. However, the mechanism of action of plant-mediated NPs still needs exploration as this activity might also be attributed to nanomaterials and their surface functionalized plant bioactive compounds.

5. Conclusions and Future Perspectives

In conclusion, *C. roseus* and *O. tenuiflorum* were found to be good choices for the synthesis of Ag NPs. The XRD study confirmed two phases (Ag and Ag_2O_3) for Ag NPs synthesized using *O. tenuiflorum*, whereas only the pure phase of Ag NPs was confirmed in

the case of *C. roseus*. The SEM and TEM analysis confirmed spherical/spheroidal-shaped Ag NPs. FTIR analysis confirmed the presence of diverse biomolecules such as aldehyde or amide groups present in the plant extracts, which were responsible for the capping and formation of Ag NPs. Further synthesized Ag NPs inhibited *Escherichia coli* and *Bacillus subtilis* and can find application against various diseases in the future after detailed follow-up studies. Lastly, the stability of NPs and toxicological impacts on human health and the environment need further validation.

Supplementary Materials: The following supporting information can be downloaded at: <https://www.mdpi.com/article/10.3390/pr11051479/s1>, Figure S1: Antibacterial activity of *C. roseus* and *O. tenuiflorum* mediated Ag NPs.

Author Contributions: Conceptualization: A.B., N.T. and A.K.; Data curation: N.T. and A.K.; Synthesis and characterization analysis: B.P., N.T., S.S. and A.K.; Antibacterial activity: A.K. and B.P.; Data interpretation: N.T., R.A., A.K. and V.A.; Supervision: N.T. and A.B.; Writing—original draft: B.P., N.T., A.K. and S.S.; Writing—review and editing: V.A. and R.A. All authors have read and agreed to the published version of the manuscript.

Funding: This research was supported by the Ministry of AYUSH, Government of India under the AYURSWASTHYA Yojana-3988.

Data Availability Statement: Data are contained within the article.

Acknowledgments: The authors (A.B., A.K. and V.A.) are grateful to Revered Swami Ramdev and the Patanjali Research Foundation Trust for providing all the necessary facilities. Further, the authors are thankful to the Ministry of AYUSH under Grant-in-Aid for Establishment of Centre of Excellence of Renovation and Upgradation of Patanjali Ayurveda Hospital, Haridwar. Harshit Thakur, a Designer at the Patanjali Herbal Research Department, assisted the authors in designing Figure 7.

Conflicts of Interest: The authors declare no conflict of interest.

References

1. Rajoriya, P.; Misra, P.; Singh, V.K.; Shukla, P.K.; Ramteke, P.W. Green synthesis of silver nanoparticles. *Int. J. Biol. Sci.* **2017**, *7*, 7–20. [[CrossRef](#)]
2. Kumar, A.; Chandel, T.; Diwaker; Thakur, N. Predicting the magnetism, structural, thermodynamic and electronic properties of new co-based Heuslers: First principle perspective. *Philos. Mag.* **2020**, *100*, 2721–2734. [[CrossRef](#)]
3. Parashar, U.K.; Saxena, P.S.; Srivastava, A. Bioinspired synthesis of silver nanoparticles. *Dig. J. Nanomater. Biostruct.* **2009**, *4*, 159–166.
4. Roy, A. Synthesis of silver nanoparticles from medicinal plants and its biological application: A review. *Res. Rev. BioSci.* **2017**, *12*, 138.
5. Vanitha, G.; Rajavel, K.; Boopathy, G.; Veeravazhuthi, V.; Neelamegam, P. Physiochemical charge stabilization of silver nanoparticles and its antibacterial applications. *Chem. Phys. Lett.* **2017**, *669*, 71–79. [[CrossRef](#)]
6. Al-Zahrani, S.S.; Al-Garni, S.M. Biosynthesis of Silver Nanoparticles from *Allium ampeloprasum* Leaves Extract and Its Antifungal Activity. *J. Biomater. Nanobiotechnol.* **2019**, *10*, 11–25. [[CrossRef](#)]
7. Kavitha, K.; Baker, S.; Rakshith, D.; Kavitha, H.U.; Yashwantha Rao, H.C.; Harini, B.P.; Satish, S. Plants as green source towards synthesis of nanoparticles. *J. Biol. Sci.* **2013**, *2*, 66–76.
8. Zahir, A.A.; Chauhan, I.S.; Bagavan, A.; Kamaraj, C.; Elango, G.; Shankar, J.; Arjaria, N.; Roopan, S.M.; Rahuman, A.A.; Singh, N. Synthesis of nanoparticles using *Euphorbia prostrata* extract reveals a shift from apoptosis to G0/G1 arrest in *Leishmania donovani*. *Nanomed. Nanotechnol.* **2014**, *5*, 4782–4799.
9. Li, X.; Xu, H.; Chen, Z.S.; Chen, G. Biosynthesis of nanoparticles by microorganisms and their applications. *J. Nanomater.* **2011**, *2011*, 270974. [[CrossRef](#)]
10. El-Sherbiny, I.M.; Salih, E. Green Synthesis of Metallic Nanoparticles Using Biopolymers and Plant Extracts. In *Green Metal Nanoparticles: Synthesis, Characterization and Their Applications*; Suvardhan, K., Shakeel, A., Eds.; Wiley: Hoboken, NJ, USA, 2018; pp. 293–319.
11. Gokila, V.; Perarasu, V.T.; Rufina, R. Qualitative comparison of chemical and green synthesized Fe₃O₄ nanoparticles. *Adv. Nano Res.* **2021**, *10*, 71–76.
12. Gour, A.; Jain, N.K. Advances in green synthesis of nanoparticles. *Artif. Cells Nanomed. Biotechnol.* **2019**, *47*, 844–851. [[CrossRef](#)]
13. Salem, S.S.; Fouda, A. Green synthesis of metallic nanoparticles and their prospective biotechnological applications: An overview. *Biol. Trace Elem. Res.* **2021**, *199*, 344–370. [[CrossRef](#)]
14. Gericke, M.; Pinches, A. Biological synthesis of metal nanoparticles. *Hydrometallurgy* **2006**, *83*, 132–140. [[CrossRef](#)]

15. Narayanan, K.B.; Sakthivel, N. Biological synthesis of metal nanoparticles by microbes. *Adv. Colloid Interface Sci.* **2010**, *156*, 1–13. [[CrossRef](#)]
16. Singh, P.; Kim, Y.J.; Zhang, D.; Yang, D.C. Biological synthesis of nanoparticles from plants and microorganisms. *Trends Biotechnol.* **2016**, *34*, 588–599. [[CrossRef](#)]
17. Husseiny, M.I.; Abd El-Aziz, M.; Badr, Y.; Mahmoud, M.A. Biosynthesis of gold nanoparticles using *Pseudomonas aeruginosa*. *Spectrochim. Acta A Mol. Biomol. Spectrosc.* **2007**, *67*, 1003–1006. [[CrossRef](#)]
18. Yadav, A.; Kon, K.; Kratosova, G.; Duran, N.; Ingle, A.P.; Rai, M. Fungi as an efficient mycosystem for the synthesis of metal nanoparticles: Progress and key aspects of research. *Biotechnol. Lett.* **2015**, *37*, 2099–2120. [[CrossRef](#)]
19. Siddiqi, K.S.; Husen, A. Fabrication of metal nanoparticles from fungi and metal salts: Scope and application. *Nanoscale Res. Lett.* **2016**, *11*, 98. [[CrossRef](#)]
20. Mishra, A.; Tripathy, S.K.; Yun, S.I. Bio-synthesis of gold and silver nanoparticles from *Candida guilliermondii* and their antimicrobial effect against pathogenic bacteria. *J. Nanosci. Nanotechnol.* **2011**, *11*, 243–248. [[CrossRef](#)]
21. Narayanan, K.B.; Sakthivel, N. Green synthesis of biogenic metal nanoparticles by terrestrial and aquatic phototrophic and heterotrophic eukaryotes and biocompatible agents. *Adv. Colloid. Interface. Sci.* **2011**, *169*, 59–79. [[CrossRef](#)]
22. Balkrishna, A.; Kumar, A.; Arya, V.; Rohela, A.; Verma, R.; Nepovimova, E.; Krejcar, O.; Kumar, D.; Thakur, N.; Kuca, K. Phytoantioxidant functionalized nanoparticles: A green approach to combat nanoparticle-induced oxidative stress. *Oxid. Med. Cell. Longev.* **2021**, *2021*, 3155962. [[CrossRef](#)]
23. Balkrishna, A.; Arya, V.; Rohela, A.; Kumar, A.; Verma, R.; Kumar, D.; Nepovimova, E.; Kuca, K.; Thakur, N.; Thakur, N.; et al. Nanotechnology interventions in the management of COVID-19: Prevention, Ddiagnosis and virus-like particle vaccines. *Vaccines* **2021**, *9*, 1129. [[CrossRef](#)]
24. Silva, L.P.; Reis, I.G.; Bonatto, C.C. Green Synthesis of Metal Nanoparticles by Plants: Current Trends and Challenges. In *Green Processes for Nanotechnology*; Basiuk, V., Basiuk, E., Eds.; Springer: Cham, Switzerland, 2015; pp. 259–275.
25. Bhembe, Y.A.; Lukhele, L.P.; Hlekelele, L.; Ray, S.S.; Sharma, A.; Vo, D.V.N.; Dlamini, L.N. Photocatalytic degradation of nevirapine with a heterostructure of few-layer black phosphorus coupled with niobium (V) oxide nanoflowers (FL-BP@Nb₂O₅). *Chemosphere* **2020**, *261*, 128159. [[CrossRef](#)]
26. Solgi, M.; Taghizadeh, M. Biogenic Synthesis of Metal Nanoparticles by Plants. In *Biogenic Nano-Particles and Their Use in Agro-Ecosystems*; Ghorbanpour, M., Bhargava, P., Varma, A., Choudhary, D., Eds.; Springer: Singapore, 2020; pp. 593–606.
27. Paul, B.; Bhuyan, B.; Purkayastha, D.D.; Dey, M.; Dhar, S.S. Green synthesis of gold nanoparticles using *Pogostemon benghalensis* (B) O. Ktz. leaf extract and studies of their photocatalytic activity in degradation of methylene blue. *Mater. Lett.* **2015**, *148*, 37–40. [[CrossRef](#)]
28. Kopaczyk, J.M.; Warguła, J.; Jelonek, T. The variability of terpenes in conifers under developmental and environmental stimuli. *Environ. Exp. Bot.* **2020**, *180*, 104197. [[CrossRef](#)]
29. Ndaba, B.; Roopnarain, A.; Haripriya, R.A.; Maaaza, M. Biosynthesized metallic nanoparticles as fertilizers: An emerging precision agriculture strategy. *J. Integr. Agric.* **2022**, *21*, 1225–1242. [[CrossRef](#)]
30. Firdhouse, M.J.; Lalitha, P.; Shubashini, S.K. Novel synthesis of silver nanoparticles using leaf ethanol extract of *Pisonia grandis* (R. Br). *Der Pharma Chem.* **2012**, *4*, 2320–2326.
31. Thakur, B.K.; Kumar, A.; Kumar, D. Green synthesis of titanium dioxide nanoparticles using *Azadirachta indica* leaf extract and evaluation of their antibacterial activity. *S. Afr. J. Bot.* **2019**, *124*, 223–227. [[CrossRef](#)]
32. Khatana, C.; Kumar, A.; Alruways, M.W.; Khan, N.; Thakur, N.; Kumar, D.; Kumari, A. Antibacterial potential of zinc oxide nanoparticles synthesized using *Aloe vera* (L.) Burm. f.: A green approach to combat drug resistance. *J. Appl. Microbiol.* **2021**, *15*, 1907–1914.
33. Thakur, N.; Kumar, K.; Kumar, A. Effect of (Ag, Zn) co-doping on structural, optical and bactericidal properties of CuO nanoparticles synthesized by a microwave-assisted method. *Dalton Trans.* **2021**, *50*, 6188–6203. [[CrossRef](#)]
34. Anand, K.; Kaur, J.; Singh, R.C.; Thangaraj, R. Preparation and characterization of Ag-doped In₂O₃ nanoparticles gas sensor. *Chem. Phys. Lett.* **2017**, *682*, 140–146. [[CrossRef](#)]
35. Ip, M.; Lui, S.L.; Poon, V.K.; Lung, I.; Burd, A. Antimicrobial activities of silver dressings: An in vitro comparison. *J. Med. Microbiol.* **2006**, *55*, 59–63. [[CrossRef](#)]
36. Thakur, N.; Thakur, N.; Chauhan, P.; Sharma, D.P.; Kumar, A.; Jeet, K. Futuristic role of nanoparticles for treatment of COVID-19. *Biomater. Polymers Horizon.* **2022**, *1*, 1–22. [[CrossRef](#)]
37. Kumar, M.; Upadhyay, L.S.; Kerketta, A.; Vasanth, D. Extracellular Synthesis of Silver Nanoparticles Using a Novel Bacterial Strain *Kocuria rhizophila* BR-1: Process Optimization and Evaluation of Antibacterial Activity. *Bionanoscience* **2022**, *12*, 423–438. [[CrossRef](#)]
38. Begum, I.; Ameen, F.; Soomro, Z.; Shamim, S.; AlNadhari, S.; Almansob, A.; Al-Sabri, A.; Arif, A. Facile fabrication of malonic acid capped silver nanoparticles and their antibacterial activity. *J. King Saud Univ. Sci.* **2021**, *33*, 101231. [[CrossRef](#)]
39. Mani, M.; Okla, M.K.; Selvaraj, S.; Kumar, A.R.; Kumaresan, S.; Muthukumaran, A.; Kaviyarasu, K.; El-Tayeb, M.A.; Elbadawi, Y.B.; Almaary, K.S.; et al. A novel biogenic *Allium cepa* leaf mediated silver nanoparticles for antimicrobial, antioxidant, and anticancer effects on MCF-7 cell line. *Environ. Res.* **2021**, *198*, 111199. [[CrossRef](#)]
40. Prabhu, S.; Poulouse, E.K. Silver nanoparticles: Mechanism of antimicrobial action, synthesis, medical applications, and toxicity effects. *Int. Nano Lett.* **2012**, *2*, 32. [[CrossRef](#)]

41. POWO. KewScience-Plants of the World Online Home Page. Available online: <https://powo.science.kew.org> (accessed on 7 April 2023).
42. Kumar, S.; Singh, B.; Singh, R. *Catharanthus roseus* (L.) G. Don: A review of its ethnobotany, phytochemistry, ethnopharmacology and toxicities. *J. Ethnopharmacol.* **2022**, *284*, 114647.
43. Lahare, R.P.; Yadav, H.S.; Bisen, Y.K.; Dashahre, A.K. Estimation of total phenol, flavonoid, tannin and alkaloid content in different extracts of *Catharanthus roseus* from Durg district, Chhattisgarh, India. *Sch. Bull.* **2021**, *7*, 1–6. [[CrossRef](#)]
44. Mandal, A.K.; Poudel, M.; Neupane, N.P.; Verma, A. Phytochemistry, pharmacology, and applications of *Ocimum sanctum* (Tulsi). In *Edible Plants in Health and Diseases: Volume II: Phytochemical and Pharmacological Properties*; Masoodi, M.H., Rehman, M.U., Eds.; Springer Nature: Singapore, 2022; pp. 135–174.
45. Chaudhary, A.; Sharma, S.; Mittal, A.; Gupta, S.; Dua, A. Phytochemical and antioxidant profiling of *Ocimum sanctum*. *J. Food Sci. Technol.* **2020**, *57*, 3852–3863. [[CrossRef](#)]
46. Kuppurangan, G.; Karuppasamy, B.; Nagarajan, K.; Krishnasamy, S.R.; Viswaprakash, N.; Ramasamy, T. Biogenic synthesis and spectroscopic characterization of silver nanoparticles using leaf extract of *Indoneesiella echioides*: In Vitro assessment on antioxidant, antimicrobial and cytotoxicity potential. *Appl. Nanosci.* **2016**, *6*, 973–982.
47. Mourdikoudis, S.; Pallares, R.M.; Thanh, N.T. Characterization techniques for nanoparticles: Comparison and complementarity upon studying nanoparticle properties. *Nanoscale.* **2018**, *10*, 12871–12934. [[CrossRef](#)]
48. M2-A5; Performance Standard for Antimicrobial Disc Susceptibility Test. Approved Standard. National Committee for Clinical Laboratory (NCCL) Standards Publication: Villanova, PA, USA, 1993.
49. CLSI Document M7-A7; Methods for Dilution Antimicrobial Susceptibility Tests for Bacteria that Grow Aerobically. Approved Standard—Seventh Addition. Clinical and Laboratory Standards Institute (CLSI): Wayne, PA, USA, 2006; ISBN 1-56238-587-9.
50. Logaranjan, K.; Raiza, A.J.; Gopinath, S.C.; Chen, Y.; Pandian, K. Shape and size-controlled synthesis of silver nanoparticles using *Aloe vera* plant extract and their antimicrobial activity. *Nanoscale Res. Lett.* **2016**, *11*, 520. [[CrossRef](#)]
51. Janardhanan, R.; Karuppaiah, M.; Hebbalkar, N.; Rao, T.N. Synthesis and surface chemistry of nano silver particles. *Polyhedron* **2009**, *28*, 2522–2530. [[CrossRef](#)]
52. Femi-Adepoju, A.G.; Dada, A.O.; Otun, K.O.; Adepoju, A.O.; Fatoba, O.P. Green synthesis of silver nanoparticles using terrestrial fern (*Gleichenia pectinata* (Willd.) C. Presl.): Characterization and antimicrobial studies. *Heliyon* **2019**, *5*, e01543. [[CrossRef](#)]
53. Verma, S.K.; Jha, E.; Sahoo, B.; Panda, P.K.; Thirumurugan, A.; Parashare, S.K.S.; Suar, M. Mechanistic insight into the rapid one-step facile biofabrication of antibacterial silver nanoparticles from bacterial release and their biogenicity and concentration-dependent in vitro cytotoxicity to colon cells. *RSC Adv.* **2017**, *7*, 40034–40045. [[CrossRef](#)]
54. Banerjee, P.; Satapathy, M.; Mukhopahayay, A.; Das, P. Leaf extract mediated green synthesis of silver nanoparticles from widely available Indian plants: Synthesis, characterization, antimicrobial property and toxicity analysis. *Bioresour. Bioprocess.* **2014**, *1*, 3. [[CrossRef](#)]
55. Ankamwar, B.; Damle, C.; Ahmad, A.; Sastry, M. Biosynthesis of gold and silver nanoparticles using *Embllica officinalis* fruit extract, their phase transfer and transmetallation in an organic solution. *J. Nanosci. Nanotechnol.* **2005**, *5*, 1665–1671. [[CrossRef](#)]
56. Kumar, S.; Singh, M.; Halder, D.; Mitra, A. *Lippia javanica*: A cheap natural source for the synthesis of antibacterial silver nanocolloid. *Appl. Nanosci.* **2016**, *6*, 1001–1007. [[CrossRef](#)]
57. Ahmed, S.; Ikram, S. Silver nanoparticles: One pot green synthesis using *Terminalia arjuna* extract for biological application. *J. Nanomed. Nanotechnol.* **2015**, *6*, 4.
58. Kumar, V.; Yadav, S.C.; Yadav, S.K. *Syzygium cumini* leaf and seed extract mediated biosynthesis of silver nanoparticles and their characterization. *J. Chem. Technol. Biotechnol.* **2010**, *85*, 1301–1309. [[CrossRef](#)]
59. Saxena, A.; Tripathi, R.M.; Zafar, F.; Singh, P. Green synthesis of silver nanoparticles using aqueous solution of *Ficus benghalensis* leaf extract and characterization of their antibacterial activity. *Mater. Lett.* **2012**, *67*, 91–94. [[CrossRef](#)]
60. Jamil, K.; Khattak, S.H.; Farrukh, A.; Begum, S.; Riaz, M.N.; Muhammad, A.; Kamal, T.; Taj, T.; Khan, I.; Riaz, S.; et al. Biogenic synthesis of silver nanoparticles using *Catharanthus roseus* and its cytotoxicity effect on vero cell lines. *Molecules* **2022**, *27*, 6191. [[CrossRef](#)]
61. Ramteke, C.; Chakrabarti, T.; Sarangi, B.K.; Pandey, R.A. Synthesis of silver nanoparticles from the aqueous extract of leaves of *Ocimum sanctum* for enhanced antibacterial activity. *J. Chem.* **2013**, *2013*, 278925. [[CrossRef](#)]
62. Palaniappan, N.; Cole, I.; Caballero-Briones, F.; Manickam, S.; Thomas, K.J.; Santos, D. Experimental and DFT studies on the ultrasonic energy-assisted extraction of the phytochemicals of *Catharanthus roseus* as green corrosion inhibitors for mild steel in NaCl medium. *RSC Adv.* **2020**, *10*, 5399–5411. [[CrossRef](#)]
63. Mandal, S.; Bhattacharya, S.R. UV-VIS and FTIR spectroscopic analysis of phytochemicals and functional group in *Ocimum sanctum* and a few medicinal plants. *Rom. J. Biophys.* **2015**, *25*, 247–257.
64. Pham, H.N.T.; Vuong, Q.V.; Bowyer, M.C.; Scarlett, C.J. Phytochemicals derived from *Catharanthus roseus* and their health benefits. *Technologies* **2020**, *8*, 80. [[CrossRef](#)]
65. Velmurugan, P.; Iydroose, M.; Lee, S.M.; Cho, M.; Park, J.H.; Balachandar, V.; Oh, B.T. Synthesis of silver and gold nanoparticles using cashew nut shell liquid and its antibacterial activity against fish pathogens. *Indian J. Microbiol.* **2014**, *54*, 196–202. [[CrossRef](#)]
66. Rautela, A.; Rani, J. Green synthesis of silver nanoparticles from *Tectona grandis* seeds extract: Characterization and mechanism of antimicrobial action on different microorganisms. *J. Anal. Sci. Technol.* **2019**, *10*, 5. [[CrossRef](#)]

67. Sarwar, A.; Katas, H.; Samsudin, S.N.; Zin, N.M. Regioselective sequential modification of chitosan via azide-alkyne click reaction: Synthesis, characterization, and antimicrobial activity of chitosan derivatives and nanoparticles. *PLoS ONE* **2015**, *10*, e0123084. [[CrossRef](#)]
68. Wang, L.; Hu, C.; Shao, L. The antimicrobial activity of nanoparticles: Present situation and prospects for the future. *Int. J. Nanomed.* **2017**, *12*, 1227. [[CrossRef](#)]
69. Manikandan, V.; Velmurugan, P.; Park, J.H.; Chang, W.S.; Park, Y.J.; Jayanthi, P.; Oh, B.T. Green synthesis of silver oxide nanoparticles and its antibacterial activity against dental pathogens. *3 Biotech* **2017**, *7*, 72. [[CrossRef](#)]
70. Levy, S.B. Active efflux mechanisms for antimicrobial resistance. *Antimicrob. Agents Chemother.* **1992**, *36*, 695–703. [[CrossRef](#)]
71. Savjani, J.K.; Gajjar, A.K.; Savjani, K.T. Mechanisms of resistance: Useful tool to design antibacterial agents for drug-resistant bacteria. *Mini. Rev. Med. Chem.* **2009**, *9*, 194–205. [[CrossRef](#)]
72. Osei Sekyere, J.; Govinden, U.; Bester, L.A.; Essack, S.Y. Colistin and tigecycline resistance in carbapenemase-producing Gram-negative bacteria: Emerging resistance mechanisms and detection methods. *J. Appl. Microbiol.* **2016**, *121*, 601–617. [[CrossRef](#)]
73. Sekyere, J.O.; Govinden, U.; Essack, S. The molecular epidemiology and genetic environment of carbapenemases detected in Africa. *Microb. Drug Resist.* **2016**, *22*, 59–68. [[CrossRef](#)]
74. Balkrishna, A.; Rohela, A.; Kumar, A.; Kumar, A.; Arya, V.; Thakur, P.; Oleksak, P.; Krejcar, O.; Verma, R.; Kumar, D.; et al. Mechanistic insight into antimicrobial and antioxidant potential of *Jasminum* species: A herbal approach for disease management. *Plants*. **2021**, *10*, 1089. [[CrossRef](#)]
75. Dakal, T.C.; Kumar, A.; Majumdar, R.S.; Yadav, V. Mechanistic basis of antimicrobial actions of silver nanoparticles. *Front. Microbiol.* **2016**, *7*, 1831. [[CrossRef](#)]
76. Jamdagni, P.; Sidhu, P.K.; Khatri, P.; Nehra, K.; Rana, J.S. Metallic Nanoparticles: Potential Antimicrobial and Therapeutic Agents. In *Advances in Animal Biotechnology and Its Applications*; Gahlawat, S.K., Duhan, J.S., Salar, R.K., Siwach, P., Kumar, S., Kaur, P., Eds.; Springer Nature: Singapore, 2018; pp. 143–160.
77. Bhardwaj, K.; Dhanjal, D.S.; Sharma, A.; Nepovimova, E.; Kalia, A.; Thakur, S.; Bhardwaj, S.; Chopra, C.; Singh, R.; Verma, R.; et al. Conifer-derived metallic nanoparticles: Green synthesis and biological applications. *Int. J. Mol. Sci.* **2020**, *21*, 9028. [[CrossRef](#)]
78. Sharmin, S.; Rahaman, M.M.; Sarkar, C.; Atolani, O.; Islam, M.T.; Adeyemi, O.S. Nanoparticles as antimicrobial and antiviral agents: A literature-based perspective study. *Heliyon* **2021**, *7*, e06456. [[CrossRef](#)]
79. Durán, N.; Durán, M.; De Jesus, M.B.; Seabra, A.B.; Fávaro, W.J.; Nakazato, G. Silver nanoparticles: A new view on mechanistic aspects on antimicrobial activity. *Nanomedicine* **2016**, *12*, 789–799. [[CrossRef](#)]
80. Slavin, Y.N.; Asnis, J.; Hñfeli, U.O.; Bach, H. Metal nanoparticles: Understanding the mechanisms behind antibacterial activity. *J. Nanobiotechnol.* **2017**, *15*, 65. [[CrossRef](#)]
81. Yin, I.X.; Zhang, J.; Zhao, I.S.; Mei, M.L.; Li, Q.; Chu, C.H. The antibacterial mechanism of silver nanoparticles and its application in dentistry. *Int. J. Nanomed.* **2020**, *15*, 2555–2562. [[CrossRef](#)]
82. Das Mahapatra, A.; Patra, C.; Mondal, J.; Sinha, C.; Chandra Sadhukhan, P.; Chattopadhyay, D. Silver nanoparticles derived from *Albizia lebbek* bark extract demonstrate killing of multidrug-resistant bacteria by damaging cellular architecture with antioxidant activity. *Chemistryselect* **2020**, *5*, 4770–4777. [[CrossRef](#)]

Disclaimer/Publisher's Note: The statements, opinions and data contained in all publications are solely those of the individual author(s) and contributor(s) and not of MDPI and/or the editor(s). MDPI and/or the editor(s) disclaim responsibility for any injury to people or property resulting from any ideas, methods, instructions or products referred to in the content.